Molecular Genetics and Metabolism Reports 33 (2022) 100914

Contents lists available at ScienceDirect

Molecular Genetics and Metabolism Reports

journal homepage: www.elsevier.com/locate/ymgmr

Generation of GLA-knockout human embryonic stem cell lines to model peripheral neuropathy in Fabry disease

Christine R. Kaneski *, John A. Hanover, Ulrike H. Schueler Hoffman

National Institute of Diabetes and Digestive and Kidney Diseases, National Institutes of Health, Bethesda, MD 20892, USA

ARTICLE INFO

Keywords:
Alpha-galactosidase
CRISPR-Cas9
Fabry disease
Human embryonic stem cells
Sensory neurons
Neuropathy

ABSTRACT

Fabry disease is an X-linked glycolipid storage disorder caused by mutations in the *GLA* gene which result in a deficiency in the lysosomal enzyme alpha galactosidase A (AGA). As a result, the glycolipid substrate Gb3 accumulates in critical tissues and organs producing a progressive debilitating disease. In Fabry disease up to 80% of patients experience life-long neuropathic pain that is difficult to treat and greatly affects their quality of life. The molecular mechanisms by which deficiency of AGA leads to neuropathic pain are not well understood, due in part to a lack of *in vitro* models that can be used to study the underlying pathology at the cellular level. Using CRISPR-Cas9 gene editing, we generated two clones with mutations in the *GLA* gene from a human embryonic stem cell line. Our clonal cell lines maintained normal stem cell morphology and markers for pluripotency, and showed the phenotypic characteristics of Fabry disease including absent AGA activity and intracellular accumulation of Gb3. Mutations in the predicted locations in exon 1 of the *GLA* gene were confirmed. Using established techniques for dual-SMAD inhibition/WNT activation, we were able to show that our AGA-deficient clones, as well as wild-type controls, could be differentiated to peripheral-type sensory neurons that express pain receptors. This genetically and physiologically relevant human model system offers a new and promising tool for investigating the cellular mechanisms of peripheral neuropathy in Fabry disease and may assist in the development of new therapeutic strategies to help lessen the burden of this disease.

1. Introduction

Fabry disease (OMIM: 301500) is an X-linked lysosomal storage disorder in which loss of function mutations in the *GLA* gene encoding for the enzyme alpha galactosidase A (AGA, EC 3.2.1.22) causes a deficiency of this enzyme [1], resulting in the accumulation of its glycolipid substrate, globotriaosylceramide (Gb3), in critical tissues and organs. Fabry disease is a progressive debilitating disorder affecting multiple organ systems with an estimated incidence of ~1 in 40,000 males [2]. However, researchers who analyzed dried blood spots collected from 34,736 newborns in an Austrian newborn screening program detected Fabry disease in 1 in 3859 births [3], suggesting this disease is under diagnosed. In its classic form, Fabry disease includes signs and symptoms such as angiokeratoma, corneal clouding, reduced sweating, hearing loss, abdominal pain, diarrhea, neuropathic pain, cardiac hypertrophy, progressive kidney failure, and stroke; and causes significant morbidity even in childhood.

One of the most debilitating symptoms of Fabry disease is pain. Two types have been described: episodic crises and constant discomfort. Many patients experience a constant burning pain in the palms of their hands and soles of their feet that is difficult to control with pain medication [4]. In addition, they may have recurrent attacks of excruciating pain ("Fabry pain crises") that occur spontaneously or in response to extreme temperatures, fever, fatigue, stress, overheating, or exercise [5]. Although enzyme replacement therapy (ERT) with AGA is currently available to treat Fabry disease, even long-term treatment does not

Abbreviations: 4-MU, 4-methylumbelliferone; AGA, alpha-galactosidase A; BRN3A, brain-specific homeobox/POU domain protein 3A; BDNF, brain-derived neurotrophic factor; DAPI, 4′,6-diamidino-2-phenylindole; DRG, dorsal root ganglion; EDTA, ethylene diamine tetracetic acid; ERT, enzyme replacement therapy; GAPDH, glyceraldehyde-3-phosphate dehydrogenase; Gb3, globotriaosylceramide; GDNF, glia-derived neurotrophic factor; eGFP, green fluorescent protein; *GLA*, alpha-galactosidase A gene; hESC, human embryonic stem cell; HEX, beta-hexosaminidase; iPSC, induced pluripotent stem cell; NGF, nerve growth factor; PAM, protospacer adjacent motif; PBS, phosphate buffered saline; RNP, ribonucleoprotein; SgRNA, single guide RNA; TNA-alpha, Tumor Necrosis Factor- alpha; TRPV1, transient receptor potential vanilloid family-1.

* Corresponding author at: National Institutes of Health, Bldg. 8, Room B122, Bethesda, MD 20892, USA.
E-mail address: Christine.Kaneski@nih.gov (C.R. Kaneski).

https://doi.org/10.1016/j.ymgmr.2022.100914
Received 31 May 2022; Received in revised form 22 August 2022; Accepted 24 August 2022

reverse the neurologic dysfunction found in these patients [6], with over 80% of patients treated with ERT reporting moderate to severe pain [7].

The pathophysiology of pain in Fabry disease is still poorly understood. Studies in patients have indicated it is a small fiber neuropathy, with large fibers largely being spared (see [8,9] for reviews). Sensory neurons respond to potentially damaging stimuli by sending signals to the spinal cord and brain. The cell bodies of these nociceptor neurons are located in the dorsal root ganglia (DRG) of the spinal cord. Neuronal storage of Gb3 has been found in DRG of patients with Fabry disease at autopsy [10], in DRG of a Fabry disease mouse model [11,12], and in the peripheral nerves of a Fabry rat model [13], and it has been suggested that this storage contributes to the neuropathic pain. In addition to direct interference with lysosomal function, accumulation of Gb3 has been shown to increase the expression of the pro-inflammatory cytokine tumor necrosis factor-alpha (TNF-alpha) in a human monocyte cell line [14]. Furthermore, expression of TNF-alpha has been shown to be elevated in peripheral blood mononuclear cells isolated from Fabry patients experiencing pain compared to normal controls [15]. Recent studies in skin fibroblasts derived from Fabry patients [16] and in a murine model of Fabry disease [17] indicated that cellular accumulation of Gb3 altered expression and function of pain-associated ion channels and expression of cytokines linked to inflammation. These results suggest that Gb3 accumulation may induce a pro-inflammatory state that potentially sensitizes the peripheral neurons to pain.

In addition, Choi and co-workers [18] reported that exposure to lyso-Gb3, a deacylated derivative of the Gb3 molecule found in high concentrations in the plasma of Fabry patients, increased pain response when applied to the foot pads of healthy mice and increased intracellular Ca^{2+} levels in a sub-population of cultured murine DRG neurons responsible for sensing damage. These results suggest metabolites of Gb3 may also contribute to pain sensitization in Fabry patients. In a study of three families with a history of Fabry disease [19], the variability in the degree of neuropathy experienced by members of the same family with identical GLA mutations suggests that genetic polymorphisms and environmental factors may alter the physiological response to Gb3 accumulation in individual patients [19], resulting in changes in sensitivity of the nociceptors to pain.

Attempts to study the pathology of Fabry-associated neuropathic pain on a molecular level have only recently been reported (see [20] for a review), in part due to the lack of relevant model systems. Several groups have used primary cultures of DRG neurons from Fabry mouse [12,18,21] and rat [13] models to study functional and morphologic changes in isolated neuronal cultures. However, primary DRG cultures are technically challenging, do not proliferate, and require the continuous maintenance of an animal colony for source tissues. In addition, although there are many similarities between human and rodent nociceptors, there are also important differences in ion channel expression and function [22].

Within the last decade there has been rapid progress in the development of techniques for the use of human pluripotent stem cells to model human diseases. Although several induced pluripotent stem cell (iPSC) lines have been generated from patients affected with Fabry disease [23–30], a major limitation of these models is that affected and control cell lines have variable genetic backgrounds which may mask subtle disease effects [31–33].

With the emergence of gene-editing techniques using the CRISPR-Cas9 system, it is now possible to target specific genes to create cellular models of human diseases that can be compared to unedited isogenic controls, considerably reducing experimental variability. In addition, methods for rapidly and reproducibly generating peripheral neurons with nociceptive properties from pluripotent stem cells using dual-SMAD inhibition/WNT activation-based methods are well established [34–37]. To create an *in vitro* model system of Fabry disease nociceptor peripheral neurons, we used CRISPR-Cas9 gene editing in a human embryonic stem cell line to generate two stable clonal cell lines, each with a complete knockout of AGA activity. We demonstrated that these lines have the phenotypic characteristics of cells derived from Fabry patients and they can be rapidly differentiated with small molecules to neurons with characteristics of nociceptors. These cell lines offer a new and promising *in vitro* model that can be used to study the cellular mechanisms of peripheral neuropathy in Fabry disease, as well as provide a tool to develop new therapeutic strategies.

2. Materials and methods

2.1. Cell culture

A human embryonic stem cell line (hESC) with a normal male karyotype, WA14 (NIHhESC-10-0064), was obtained at passage 18 from the WiCell Research Institute (Madison, WI) and was used with institutional approval.

Cultures were expanded and maintained in a feeder-free system in 6-well plates coated with Matrigel substrate (Corning, Glendale, AZ) in TeSR™-E8™ medium (StemCell Technologies, Cambridge, MA) and were routinely passaged at a 1:6 ratio when they were 60% to 80% confluent using phosphate buffered saline containing EDTA (0.5 mM) according to the method of Beers et al. [38]. After passage 32, culture medium was changed to mTeSR™ Plus (StemCell Technologies) for routine maintenance.

2.2. Generation of GLA knockout cells using ribonucleoprotein (RNP) complexes

Three CRISPRevolution Synthetic RNA kits consisting of chemically modified simple guide RNAs (SgRNA) that targeted three different potential CRISPR sites in exon 1 of the human GLA gene were provided by Synthego (Redwood City, CA). Sequences for each SgRNA were derived from the human mRNA for alpha-galactosidase A (GeneBank X05790.1) (Table 1).

In two separate experiments, WA14 cells at passage 30 or 31 were resuspended as single cells using Accutase™ cell detachment solution (Stem Cell Technologies), washed 4 times with Opti-MEM + 10 uM Y27632 (BioGems, Westlake Village, CA), and seeded on Matrigel-coated plates in TeSR™-E8™ medium with 10 uM Y27632. Each SgRNA was complexed with GenCRISPR NLS-Cas9-EGFP Nuclease (GeneScript, Piscataway, NJ) in Opti-MEM medium and the cells were transfected with the RNP complexes using TransIT-X2® Dynamic Delivery System (Mirus Bio LLC, Madison, WI). Transfections were performed in duplicate. After 24 h, one well was used to monitor transfection efficiency by fluorescence microscopy using a Zeiss Axiovert microscope (Dublin, CA) and by flow cytometry using the FL1 channel of a FACSCalibur flow cytometer (BD Biosciences, San Jose, CA). To avoid exposing cells to possible mutagenesis from UV light, a separate well was used to generate single cell clones.

To generate the WA14 clone designated 01–56, a washed, single-cell suspension of WA14 cells at p30 was seeded in Matrigel-coated 24-well

Table 1
SgRNA used for WA14 CRISPR-Cas9 editing.

Designation	Synthego RNA Name	Sequence	GLA EX1 mRNA target nucleotide numbers
SgRNA #1	GLA-101407798	5'-UAGAGCACUGGACAAUGGAU-3'	110–129
SgRNA #2	GLA-101407831	5'-UCUAGCCCCAGGGAUGUCCC-3'	94–113
SgRNA #3	GLA-101407875	5'-AGGAACCCAGAACUACAUCU-3'	33–52

plates at approximately 67,000 cells/well and incubated overnight in TeSR™-E8™ medium with 10 uM Y27632. For each well, 12 pmoles of SgRNA #1 was complexed with 6 pmoles of GenCRISPR NLS-Cas9-EGFP Nuclease in 100 µl Opti-MEM medium in a 1.5 ml microfuge tube. RNP complexes were incubated for 15 min at 37° C and then 2 µl of TransIT-X2® transfection reagent was added to the complexes, mixed, and incubated for an additional 15 min at room temperature. After the incubation, 50 µl of transfection complexes were added to each well of a 24-well plate.

To generate the WA14 clone designated 334–04, a washed, single cell suspension of WA14 cells at p31 was seeded in Matrigel-coated 12-well plates at approximately 150,000 cells/well and allowed to attach at room temperature while the transfection complexes were being prepared. For each well, 26 pmoles of SgRNA #3 was complexed with 13 pmoles of GenCRISPR NLS-Cas9-EGFP Nuclease (GeneScript) in 80 µl Opti-MEM medium in duplicate 1.5 ml microfuge tubes. RNP complexes were incubated for 15 min at 37° C, and then 20 µl of Opti-MEM containing 2.0 µl of TransX2 transfection reagent were added to the complexes and incubated for an additional 15 min at room temperature, After incubation, the whole volume from each tube was added to one well of a 12-well plate.

There were no clones generated from cells transfected with SgRNA #2.

2.3. Flow cytometry of transfected cells

At 24 h post-transfection, one well of cells from each sample was reduced to a single cell suspension with Accutase and resuspended in FACS buffer (PBS with 0.5 mM EDTA and 0.5% BSA). PMT voltage of the FL1 channel was adjusted with untransfected wild-type controls and then 5000 cells from each sample were measured using a FACSCalibur flow cytometer. Results were analyzed with Flowing Software (Turku Bioscience, Turku, Finland).

2.4. Establishment of single cell clones from transfected cells

At 24 h post-transfection, a second well of cells was refed with MTeSR™ Plus medium. At 48 h post-transfection the cultures were reduced to a single cell suspension with Accutase, washed 4 times with Opti-MEM + 10 uM Y27632, counted, and approximately 1000–1500 cells were seeded in 100 mm Matrigel-coated culture dishes on MTeSR™ Plus medium +10 uM Y27632. Cells were maintained on MTeSR™ Plus medium +10 uM Y27632 for 4 days when small colonies appeared. Colonies were expanded on MTeSR™ Plus medium without Y27632 for an additional week. Well-isolated colonies were carefully scraped and transferred with a pipet tip to one well of a Matrigel-coated 24-well plate and were expanded in MTeSR™ Plus medium until there were sufficient cells for an AGA enzyme assay.

For cells transfected with SgRNA #3 an additional round of cloning was required. The colony with the lowest AGA activity was subcloned using MTeSR™ Plus medium supplemented with 10% CloneR supplement (Stem Cell Technologies) according to the manufacturer's directions.

2.5. Measurement of AGA activity in cell extracts

A standard fluorometric assay for AGA in cell extracts was performed as previously described [39] with modifications. Briefly, cell pellets were resuspended in citrate-phosphate buffer (pH 4.6) containing sodium taurocholate (5 mg/ml) and Triton-X 100 (0.1%). The suspensions were frozen (−20° C) and thawed once, then centrifuged at 5000 X g for 5 min. Aliquots of the supernatant were incubated in duplicate for one hour with 4-methylumbelliferyl-alpha-D-galactopyranoside (5 mM, Research Products International, Mount Prospect, IL) in citrate-phosphate buffer (pH 4.6) in the presence of *N*-acetyl-galactosamine (0.1 M, Research Products International), a specific inhibitor of alpha-*N*-acetylgalactosaminidase (alpha-galactosidase B) [40]. At the end of the incubation period, enzyme activity was stopped with glycine buffer (0.1 N, pH 10.6). Fluorescence in samples was determined using a CytoFluor 4000 plate reader (Applied Biosystems, Foster City, CA) with an excitation filter of 360 nm and emission filter of 490 nm. Amount of product formed was determined using 4-methlyumbelliferone (4MU) standards diluted in 0.1 N glycine stop buffer. Protein levels in extracts were determined using the BCA protein assay kit (Pierce, Rockford, IL) according to the manufacturer's instructions using BSA as standard. AGA activity was calculated as nmoles 4-MU formed/h/mg protein and results were compared to untransfected controls included in the same assay.

As a control for samples with deficient AGA activity, a second lysosomal hydrolase, beta-hexosaminidase (HEX), was assayed at the same time under the same conditions except 2 mM 4-methylumbelliferyl-*N*-acetyl-beta-D-glucosaminide (Sigma Chemical Company, St. Louis, MO) was used as substrate and incubation was stopped after 20 min.

2.6. Analysis of CRISPR-Cas9-induced mutations in GLA gene

Total DNA was extracted from cultured cells using a Genomic Wizard DNA Extraction Kit (Promega, Madison, WI). A 571 base pair (bp) segment flanking the CRISPR *GLA* target sites was amplified with repliQa HiFi ToughMix® (QuantaBio, Beverly, MA) according to the manufacturer's protocol using the primer pair 5'-ACGGCTATAGCGA-GACGGTA-3′ (forward) and 5'-CCTGATGCAGGAATCTGGCT-3′ (reverse). PCR products were purified with sparQ PureMag Beads, (QuantaBio), checked for quality by agarose electrophoresis, and then submitted for Sanger sequencing using the forward primer to ACGT, Inc. (Germantown, MD). Chromatograms were analyzed for mutations using the on-line Synthego ICE CRISPR Analysis Tool (https://www.synthego.com/products/bioinformatics/crispr-analysis).

2.7. Western blot analysis

Cultures were harvested with PBS/EDTA and cell pellets were extracted as described above for the AGA enzyme assay. The protein content of the extracts was determined using a BCA Assay Kit (Pierce). Extracts (10 µg per lane) and molecular weight markers (Page Ruler Plus, Thermo Scientific, Waltham, MA) were separated by SDS/PAGE using a 4–12% Bis-Tris polyacrylamide gel, transferred to a 0.45 PVDF membrane, and probed with rabbit anti-AGA antibody (a gift from Transkaryotic Therapies, Inc., Cambridge, MA) at a dilution of 1:2000 in OneBlock™ Western-CL Blocking Buffer (Genesee Scientific, El Cajon, CA). Protein bands were labeled using HRP-conjugated goat anti-rabbit IgG antibody (Millipore, Temecula, CA) and they were visualized with Clarity ECL substrate (Bio-Rad, Hercules, California). Chemiluminescence was detected with an Amersham™ 600 digital imager (GE Healthcare Life Sciences, Pittsburgh, PA). HEK-293 cells transfected with a plasmid expressing human AGA (a gift from Dr. Roscoe Brady, National Institutes of Health, Bethesda, MD) were used as positive controls.

For loading controls, blots were reprobed with mouse anti-GAPDH antibody (Thermo Fisher Scientific) at 1:2000 in OneBlock™. Protein bands were detected with HRP-labeled goat anti-mouse IgG (Millipore) followed by development with Clarity ECL substrate and digital imaging with an Amersham™ 600 digital imaging system.

2.8. Differentiation to nociceptor neurons by dual-SMAD inhibition/WNT activation

Cells were differentiated to peripheral neurons with properties of nociceptors according to the method of Chambers and co-workers [34,35]. Briefly, WA14 cells were seeded in Matrigel-coated 6-well plates in TeSR-E8 medium with 10 uM Y27632. When cultures were 60%–80% confluent, usually within 48 h, differentiation was initiated

on Day 0 by replacing culture medium with KSR medium (KnockOut™ DMEM supplemented with 20% KnockOut™ Serum Replacement, 1% L-glutamine, 1% MEM NEAA and 0.1% 2-mercaptoethanol (all from Thermo Fisher Scientific) containing 10 μM SB-431542 and 100 nM LDN-193189 (both from Tocris Bioscience, Minneapolis, MN). Medium was replenished daily. On Day 2, 3 μM CHIR 99021, 10 μM DAPT, and 5 μM SU5402 (all from Selleck Chemicals, Radnor, PA) were also added to the culture medium. Starting on Day 4, KSR culture medium was gradually replaced with N2 medium consisting of DMEM/F12 medium (Thermo Fisher Scientific) supplemented with 2 mM Glutamax™ and 1% N2 supplement (Thermo Fisher Scientific). On Day 6, SB-431542 and LDN-193189 were discontinued and the cultures were fed with CHIR 99021, DAPT, and SU5402 only until Day 12. For most experiments, cultures were disassociated with Accutase to single cells on Day 8, washed, and reseeded onto Matrigel-coated culture vessels as required for each experiment, or were viably frozen for later use as described by Hoelting et al. [41]. Differentiation was continued in the new culture vessel until Day 12. After Day 12, cultures were maintained in N2 growth medium consisting of N2 medium supplemented with 20 ng/mL brain-derived neurotrophic factor (BDNF; Alomone Labs, Jerusalem, Israel), 20 ng/mL glia-derived neurotrophic factor (GDNF; Alomone Labs), and 25–50 ng/mL nerve growth factor (NGF; PeproTech, Cranbury, NJ). Every 7–10 days, 1 μg/mL mouse laminin I (Invitrogen, Thermo Fisher Scientific) was also added to the culture medium to maintain neuronal adhesion.

2.9. Immunostaining

For immunostaining, WA14 neurons at Day 8 were seeded on 2-well glass slides coated with Matrigel and differentiated as described in Section 2.6. At Day 14–28, they were fixed for 20 min at room temperature with 3% paraformaldehyde containing 2% sucrose and stored at 4 °C in PBS until use.

Fixed cells were stained by indirect immunofluorescence. The cells were blocked in 10% normal goat serum in PBS for 1 h at room temperature, and then incubated overnight at 4° C with the indicated primary antibody diluted in 1% normal goat serum in PBS. After overnight incubation, slides were washed with PBS, and then stained with the appropriate secondary antibody conjugated with either AlexaFluor 488 (green) or AlexaFluor 594 (red). Except for SSEA-4 and TRA-1-60, 0.2% saponin was included in all incubation and washing solutions as a permeabilizing agent. In some experiments, nuclei were visualized by incubating with 300 nM 4′,6-diamidino-2-phenylindole (DAPI) in PBS for 5 min before washing. Slides were mounted in 90% glycerol in PBS with 50 mg/ml n-propylgallate as antifade reagent. Staining was imaged with a Keyence BZ-9000 fluorescence microscope (Itasca, IL) with a 20× objective. To control for non-specific staining, all immunostaining experiments included a negative control culture that was stained in parallel with primary antibody omitted. The primary antibodies used in the study are listed in Table 2.

3. Results

3.1. CRISPR-Cas9-mediated knockout of GLA expression in WA14 hESCs

To create an *in vitro* model to investigate the role of AGA deficiency in the development of peripheral neuropathy in Fabry patients, we first established an AGA-deficient cell line using CRISPR-Cas9 gene editing to disrupt the *GLA* gene in a normal male hESC line WA14. Initially, we tried to generate *GLA* knock-out clones by screening WA14 cells transfected with a multicistronic DNA plasmid expressing SgRNA, Cas9 nuclease, and a mCherry reporter using both liposomal and non-liposomal transfection reagents. Transfection efficiencies by this method were usually less than 25%, which was consistent with those reported in the literature [42]. Because we did not want to stress the cells by using flow cytometry for enrichment, and we did not want to use antibiotic selection, even transiently [43], to avoid stable integration of the plasmid, we sought a more efficient editing system to reduce the number of clones that needed to be screened to find a knock-out cell line. By transfecting WA14 cells with SgRNA complexed with eGFP-labeled Cas9 nuclease (RNP complexes), we were able to achieve transfection efficiencies of 65%–82% (Fig. 1A). We incubated the transfected cultures for48 hours post-transfection to allow the cells to recover, and then reseeded them as single cells in 100-mm dishes at a density that allowed formation of well-separated colonies. When colonies were approximately 1–2 mm, we selected a representative number, expanded them on growth medium, and screened them for AGA activity.

As shown in Fig. 1B, by using this functional assay for screening, we were able to easily group colonies as normal (> 80%), severely reduced (<10%), or mixed population (25%–75%). For WA14 cells transfected with SgRNA #1, we found 2 of 36 colonies with AGA activity that was less than 5% of normal. One, designated Clone 01–56, had undetectable AGA activity. This colony was expanded for further study. For WA14 cells transfected with SgRNA #3, 2 of 7 colonies had AGA activities, indicating a mixed population. We selected the clone with lowest AGA activity (24%) to subclone (indicated by a square in Fig. 1B). The second round of cloning confirmed this colony was composed of a mix of mutant and normal cells. Of the 24 subclones tested, 2 had AGA activities of 104% and 106%; one had an AGA activity of 23%, indicating it was still a mixed population; and the remaining 21 clones had activities from 0% to 2.0% of control. One of the subclones with undetectable activity, designated Clone 334–04, was expanded for further study. For the cells transfected with SgRNA #2, 1 of 23 clones showed an AGA activity in the mixed population range and the rest were in the normal range. None of these colonies was expanded.

3.2. Gene-edited WA14 clones display a Fabry phenotype

Chromatograms from Sanger sequencing of the PCR products flanking the DNA CRISPR target sites showed disruption of the sequence of *GLA* exon 1 in the chromosomal DNA around the predicted cut site in

Table 2
Antibodies used for immunostaining.

Antigen	Clone/Designation	Antibody Type	Dilution	Company	Location
Gb3 (CD77)	BGR-23	mouse IgG	1:300	AMSBIO	Lake Forest, CA
Oct4	PCRP-POU5F1-1A4	mouse IgG	2.0 μg/ml	Developmental Studies Hybridoma Bank	Iowa City, IA
Nanog	PCRP-NANOGP1-2D8	mouse IgG	2.5 μg/ml	Developmental Studies Hybridoma Bank	Iowa City, IA
SSEA-4	GTX48037	mouse IgG	1:250	GeneTex	Irvine, CA
TRA-1-60	TRA-1-60	mouse IgM	1:100	Ebioscience	San Diego, CA
BRN3A	LS-C291450	rabbit IgG	1:100	LSBio	Seattle WA
Islet1/ISL1	Islet1/ISL1	rabbit IgG	1:500	Sino Biological	Wayne, PA
Peripherin	Clone 8G2	mouse IgG	1:200	Sigma-Aldrich	St. Louis, MO
Tubulin, beta-III	TUJI	mouse IgG	1:500	Covance	Princeton, NJ
Tubulin, beta-III	TUBB3	rabbit IgG	1:300	Sino Biological	Wayne, PA
TRPV1	A8564	rabbit IgG	1:100	AbClonal	Woburn, MA
NAV1.7/SCN9A	*E*-AB-32156	rabbit IgG	1:500	Elabscience Biotechnology Inc	Houston, Texas
NAV1.8/SCN10A	GTX42021	mouse IgG	1:100	GeneTex	Irvine, CA

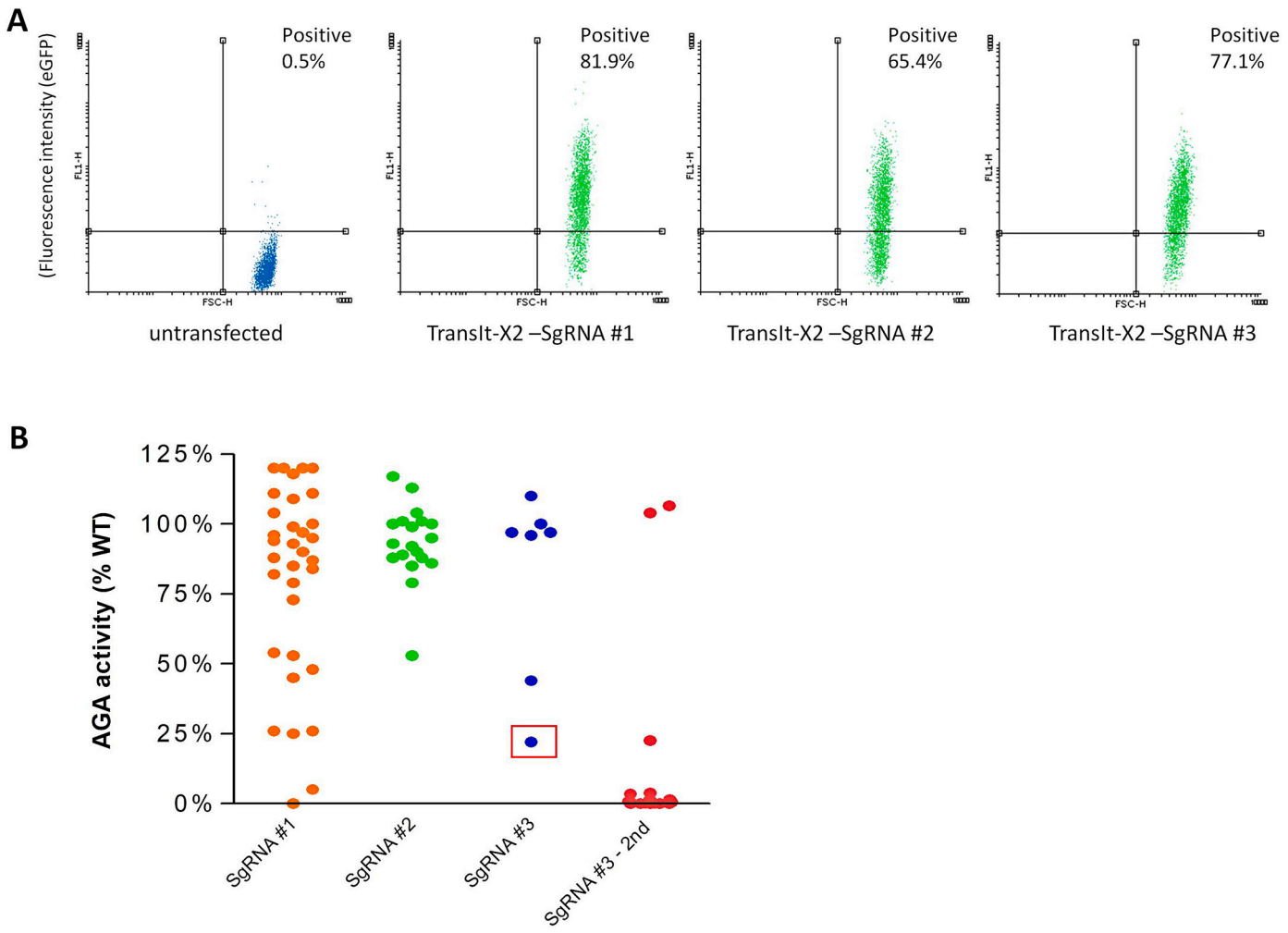

Fig. 1. CRISPR-Cas9-mediated knockout of GLA expression in WA14 cells. (A) WA14 cells were transfected with three different RNP complexes using eGFP-labeled Cas9 nuclease as described in Methods. After 24 h, cultures were resuspended as single cells and 5000 cells were analyzed in the FL1 channel of a FACSCalibur flow cytometer. A positive signal was defined as fluorescence intensity larger than 99.5% of untransfected control cells. (B) Colonies were established from RNP-transfected cells as described in Methods. Cells from approximately 2/3 of a 24-well plate were harvested with PBS/EDTA and assayed for AGA and HEX activities. Results are expressed as percent AGA activity relative to wild-type controls. Each point is a single colony. The colony from SgRNA #3 indicated with a square was subcloned to remove contamination with wild-type cells (SgRNA #3-2nd).

both clones (Fig. 2). Clone 01–56 has an in-frame 6-nucleotide deletion, and Clone 334–04 has a one base pair insertion resulting in a frame shift.

Repeated measurements of the lysosomal enzymes, AGA and HEX, made over several weeks in culture confirmed the severe deficiency in AGA activity in both clones (Fig. 3A). By contrast, the activity of the second lysosomal enzyme, HEX, was within the normal range, confirming that the lack of AGA activity was not due to a general decrease in lysosomal enzyme activity. AGA and HEX assays shown in Fig. 3A represent enzyme activity assays performed at 2, 4, and 8 weeks in culture. The lack of change in AGA activity indicated that the mutations induced in the clones remained stable over time, and the cultures were free of contaminating wild-type cells that could overgrow the culture.

Because the 6-bp deletion in Clone 01–56 was in-frame, we performed a Western blot of AGA protein to determine whether the lack of AGA activity in our clones was the result of the absence of AGA protein or the expression of a mutant protein. The results show that both clones lacked detectable levels of AGA protein compared to untransfected controls (Fig. 3B).

Fabry disease is characterized by the accumulation of the glycolipid Gb3 in the cells of Fabry patients. Therefore, we evaluated Gb3 levels in our gene-edited cell lines by immunostaining. Under our feeder-free culture conditions using MTeSR™ Plus medium, there was a significant accumulation of Gb3 in both clones compared to normal wild-type cells (Fig. 3C).

3.3. *GLA gene-edited WA14 cells retain markers of pluripotency*

To confirm that knock-out of AGA enzyme activity in WA14 cells did not affect their pluripotent potential, the expression of pluripotency markers Oct4, SSEA-4, Nanog, and TRA-1-60 was verified by immunofluorescent staining (Fig. 4). Both Clone 01–56 and Clone 334–04 were positive for these markers. In addition, both AGA-deficient clones displayed typical pluripotent morphology consisting of small tightly packed cells with a high nucleus-to-cytoplasm ratio.

3.4. *AGA-deficient WA14 clones can be differentiated into peripheral neurons with nociceptor properties*

Pluripotent stem cells can be differentiated into numerous cell types. To determine whether human embryonic stem cells with deficient AGA activity can be differentiated into pain-sensing peripheral neurons, we used dual-SMAD inhibition/WNT activation with the small molecules LDN-193189 and SB431542 combined with SU5402, CHIR99021 and DAPT to differentiate our *GLA* gene-edited clones as described in

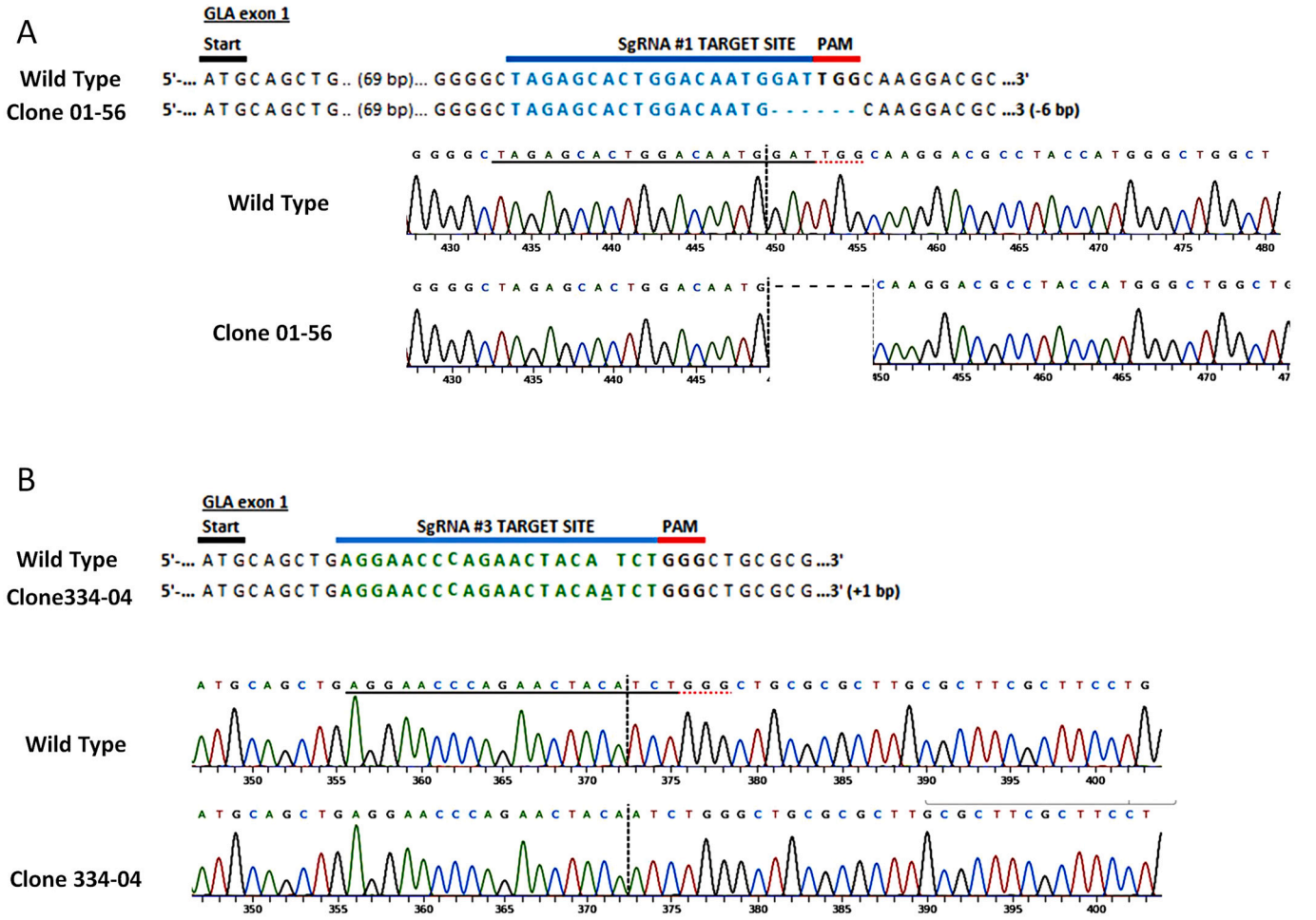

Fig. 2. Sequence of GLA exon 1 in gene-edited WA14 clones. Sequencing chromatograms and sequence alignments for WA14 Clone 01–56 (A) and Clone 334–04 (B). The AGA start codon is indicated by a black bar in the sequence alignment. The DNA sequence corresponding to the SgRNA annealing site is underlined in black in the chromatogram and indicated by a blue bar in the sequence alignment. The upstream protospacer adjacent motif (PAM) is indicated in red. The expected cut side is marked with a dotted line in the chromatograms.

Methods. After 12 days of small molecule treatment, we were able to reproducibly generate cultures with abundant numbers of neuronal-type cells from both Clone 01–56 and Clone 334–04 (Fig. 5), as well as wild-type WA14 cells (not shown).

Over the course of the 12-day differentiation procedure, cultures tended to develop neuronal clusters with processes projecting away from the clustered domains (Fig. 5A). Attempts to transfer the cells after Day 12, when the differentiation protocol was complete, met with limited success, with many of the cells detaching within 24 h after plating. Therefore, following the procedure of Hoelting and co-workers [41], at Day 8, we reduced the cultures to single cells using Accutase, counted them, and reseeded the cells in Day 8 differentiation medium in Matrigel-coated culture vessels as required for each experiment. Alternatively, the cells were frozen at this stage for later use. Following transfer, differentiation treatment for Days 9–12 was completed in the experimental dish. This procedure allowed the reliable establishment of monolayer cultures with similar cell numbers for each cell line (Fig. 5B). At the end of the small molecule treatment at Day 12, cultures could be maintained on DMEM/F12 medium with 1% N2 supplement and BDNF (20 ng/ml), GDNF (20 ng/ml) and NGF (25 ng/ml) (N2 growth medium) for up to 40 days. As cultures matured, the cells clustered into ganglia-like processes with connecting fibrils (Fig. 7C).

To confirm the neuronal phenotype of the differentiated cells, we immunostained them with markers for peripheral and sensory neurons. By Day 14, the cells developed bipolar neuronal morphology (Fig. 5B) and were positive for the pan-neuronal marker beta-III tubulin (Fig. 6) and for peripherin, a marker for peripheral neurons (Fig. 6A). The cells also showed strong, nearly homogeneous expression of two well-established markers for sensory neurons, the transcription factor brain-specific homeobox/POU domain protein 3A (BRN3A) [44] (Fig. 6B), and insulin gene enhancer protein (Islet1) [45] (Fig. 6C).

There are three main subsets of sensory neurons—proprioceptors, mechanoreceptors, and nociceptors. To determine if our neurons were nociceptors, we immunostained them for the pain channels Nav1.7 (SCN9A) and NaV1.8 (SCN10A), and vanilloid receptor TRPV1. As shown in Fig. 7, cultures were positive for all three markers. These results indicated that AGA-deficient hESC can be differentiated to sensory peripheral neurons with properties of nociceptors.

4. Discussion

In Fabry disease up to 80% of patients experience life-long neuropathic pain that is difficult to treat and greatly affects their quality of life [7]. The molecular mechanisms by which deficiency of AGA leads to neuropathic pain are not well understood, due in part to a lack of *in vitro* models that can be used to study the underlying pathology at the cellular level. Several groups have reported the use of primary neuronal cultures isolated from DRG from Fabry mouse [12,18,21] and Fabry rat [13] models to study functional and morphologic changes in isolated neuronal cultures. However, isolation of primary DRG neurons is not

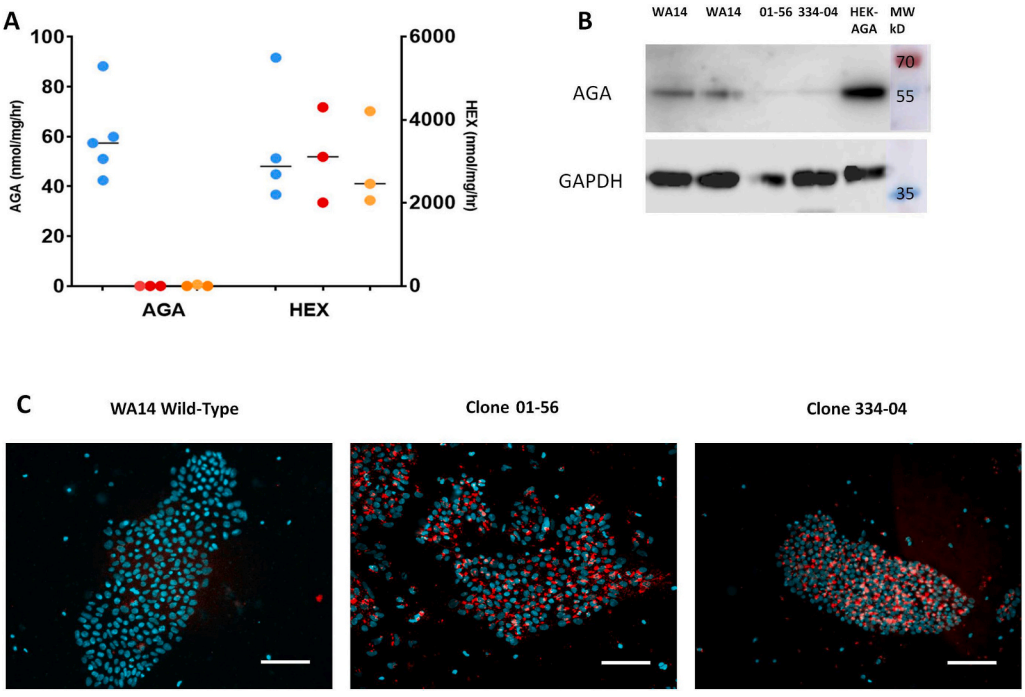

Fig. 3. Deficiency of AGA enzyme in CRISPR-Cas9 edited WA14 cells. (A) AGA and HEX enzyme activities in cellular homogenates of wild-type (blue), Clone 01–56 (orange) and Clone 334–04 (red). Results are expressed as nmol 4MU released/h/mg cell protein. Each point represents a separate assay performed in duplicate. (B) Western blot of AGA protein expression. Amount of immunoreactive AGA was severely reduced in the gene-edited clones compared to wild-type. HEK-293 cells transfected with a plasmid expressing human AGA were included as a positive control. GAPDH levels were used as a loading control. (C) Cultures of wild-type, Clone 01–56, and Clone 334–04 cells were fixed and immunostained for Gb3 (red) as described in Methods. Nuclei were counterstained with DAPI (blue) and slides were imaged in a Keyence 9000 microscope with a 20× objective. Scale bar = 100 μm.

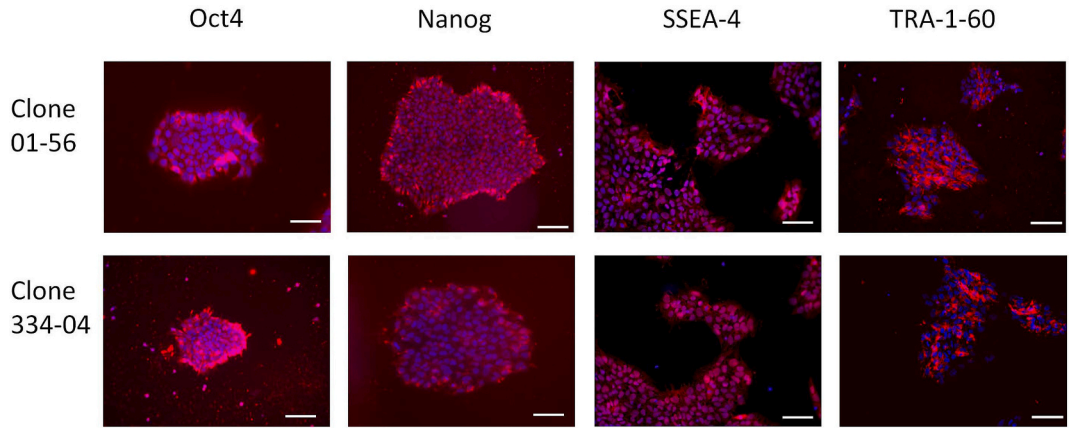

Fig. 4. Expression of markers of pluripotency in GLA gene-edited WA14 clones. Cells were seeded onto Matrigel-coated slides and immunostained as described in Methods using an Alexa-594-labeled secondary antibody (red) to detect positive staining. Nuclei were counterstained with DAPI (blue). Slides were imaged with a 20× objective in a Keyence 9000 microscope. Scale bar = 100 μm.

practical for the study of neuronal dysfunction in humans.

In order to provide a human neuronal model system, previously our group used gene-silencing by stable transfection with short-hairpin RNA targeting AGA in the human neuroblastoma cell line LA-N-2 [46] to produce two clonal cell lines with a Fabry phenotype. However, although this model has many neuronal features, it is not directly derived from peripheral neurons. Several groups have reported the development of induced pluripotent cell lines using primary cells from Fabry patients [23–30] and the use of CRISPR-Cas9 gene editing either to generate *GLA*-knockout stem cell models from the hESC cell line WA09 (H9) [47] and from normal iPSC lines [48–50], or to generate gene-corrected Fabry iPSC [50,51] to create isogenic controls. To date these pluripotent stem cell lines have been used mainly to study molecular mechanisms of cardiomyopathy found in Fabry patients [23,28,30,47,50,52], in addition to kidney [49] and vascular endothelial dysfunction [51], but to our knowledge there have been no reports of using Fabry pluripotent cells to model peripheral pain-sensing neurons.

In this paper we report the development of two new human *GLA*-knockout cell lines derived from the human embryonic stem cell line WA14 using CRISPR-Cas9 gene editing to target the *GLA* gene. We demonstrate these clones closely model the defects found in cells from Fabry patients and they can be differentiated into peripheral-type neurons with properties of nociceptors that can be used to study the molecular mechanisms of peripheral neuropathy in Fabry patients on a cellular level.

By transfecting WA14 cells with RNP complexes we were able to avoid several drawbacks of plasmid transfection. Because RNP complexes are formed from SgRNA and Cas9 nuclease, translation from a DNA template is not necessary. Gene edits occur within the first 24 h after transfection and the Cas9 protein is rapidly degraded [53], reducing the potential for off-target effects. In addition, the possibility of gene disruption due to random genetic integration of the DNA plasmid-backbone elements into the cellular DNA is eliminated. Because of the increased efficiency of transfection with RNP complexes (Fig. 1) compared to plasmids in hESC, we were able to avoid the necessity of enriching the transfected cells by flow cytometry, which can lead to

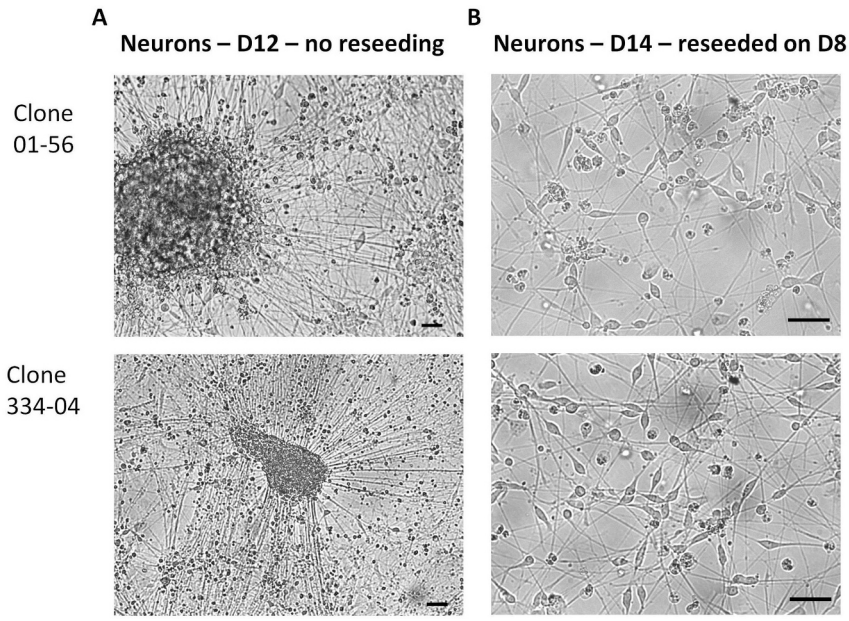

Fig. 5. Differentiation of GLA gene-edited WA14 cells into neurons. (A) Cultures were differentiated in 6-well plates as described in Methods. At Day 12, live cultures were imaged with a Zeiss Axiovert microscope using a 10× objective. Scale bar = 50 μm. (B) Single cell neuronal cultures. Cultures were differentiated as described in Methods. At Day 8, cultures were reduced to single cells and cryopreserved. Once thawed, cells were seeded on Matrigel-coated slides and differentiation was continued for an additional 4 days, followed by feeding with N2 growth medium. At Day 14, living cultures were imaged with a Zeiss Axiovert microscope using a 20× objective. Scale bar = 50 μm.

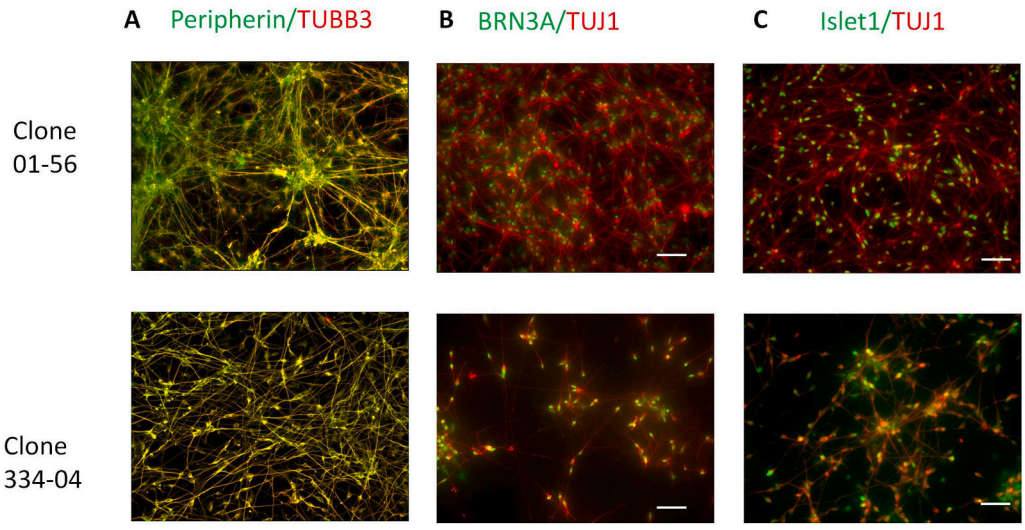

Fig. 6. Immunostaining of neuronal cells derived from AGA-deficient WA14 clones for markers of sensory neurons. WA14 clones were differentiated as described in Methods. At Day 8, they were transferred to Matrigel-coated 2-well glass chamber slides and the differentiation protocol was continued to Day 12, after which the cells were refed with N2 growth medium. At Day 14, the cultures were fixed and stained as described in Methods. (A) Cells were double stained for peripherin (green) and beta-III-tubulin (TUBB3, red). Areas of overlap appear as yellow. (B) Cells were double stained for BRN3A (green) and beta-III-tubulin (TUJ1, red). (C) Cells were double stained for Islet1 (green) and beta-III-tubulin (TUJ1, red). All slides were imaged in a Keyence 9000 microscope using a 20× objective. Scale bars = 100 μm.

shear-stress and cell death. This is especially important in mutant cells that may be physically and metabolically fragile. The efficiency of gene edits also allowed us to generate multiple clonal cell lines with the same genetic background, two of which we expanded and characterized. These clones can be used to compare results with isogenic wild-type cells as well as with each other.

Our gene-edited clones maintained expression of pluripotent stem cell markers (Fig. 4) and had the typical morphology of hESC. These AGA-deficient cell lines modeled the phenotypic characteristics of cells derived from Fabry patients. As we have shown, both WA14 Clone 01–56 and Clone 334–04 have a specific, severe reduction in lysosomal AGA enzyme activity in cell homogenates (Fig. 3A), as well as severely reduced expression of AGA protein by Western blot (Fig. 3B). Under our culture conditions, the cells accumulate Gb3 (Fig. 3C), another phenotypic marker of Fabry cells. Sanger sequencing confirmed each clone had a different genetic mutation in the predicted location in exon 1 of the *GLA* gene (Fig. 2). Because we routinely culture the cells in defined medium in the absence of feeder layers, variation in cellular metabolism due to lot-to-lot variability of the lipid content in serum can be controlled. In addition, the unknown effects of cellular interactions with inactivated, but phenotypically normal, murine fibroblasts are eliminated.

The method established by Chambers et al. [34] for differentiating pluripotent cells with a small molecule-based method for dual-SMAD inhibition/WNT activation has been shown to produce nearly pure cultures of nociceptors that are molecularly comparable to human sensory neurons derived from human DRG [36]. They are capable of responding to noxious stimuli, exhibit mature electrophysiological characteristics, and express ion channels related to the perception of pain [36,54]. Chambers et al. [28] also reported that the sodium channels SCN9A (Nav1.7), SCN10A (NaV1.8) and SCN11A, the purinergic receptor P2RX3, and the vanilloid receptors TRPV1 and TRPM8 were upregulated in differentiated cells. McDermott et al. [54] confirmed that NAV1.7 channels were highly expressed in neurons derived from normal iPSC by this method and that NAV1.7 plays a crucial role in human nociception.

Using the protocol published by Chambers et al. [35], we were able to generate large numbers of neuronal cells from normal and AGA-

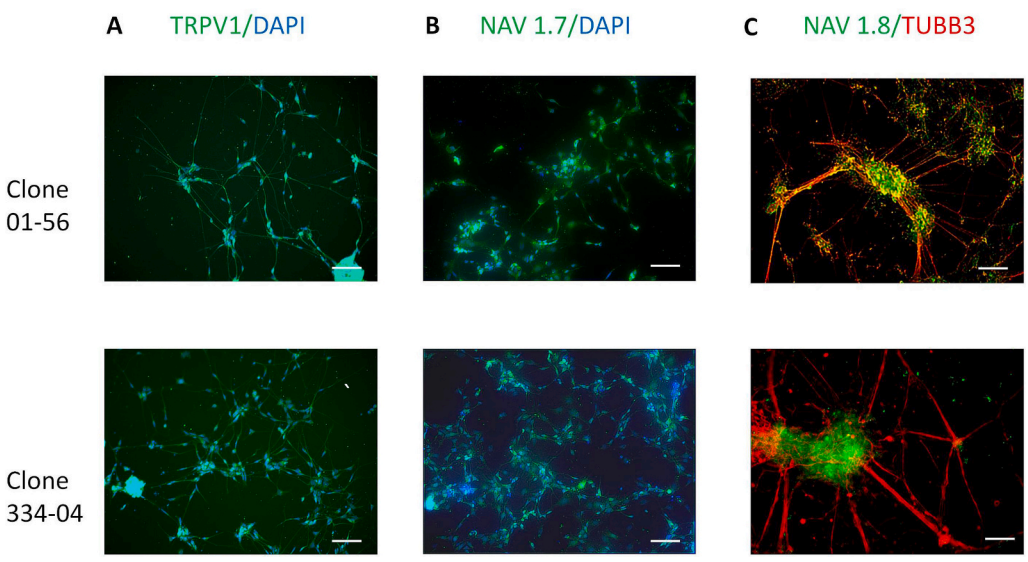

Fig. 7. Immunostaining of neuronal cells derived from AGA-deficient WA14 clones for pain receptors. WA14 clones were differentiated as described in Methods. At Day 8, they were transferred to Matrigel-coated 4-well glass chamber slides and the differentiation protocol was continued to Day 12, after which the cells were refed with N2 growth medium. At Day 21 (A and B) or Day 28 (C), the cultures were fixed and stained as described in Methods. (A) Cells were stained for TRPV1 (green). Nuclei were counterstained with DAPI (blue). (B) Cells were stained for NAV1.7 (SCN9A) (green). Nuclei were counterstained with DAPI (blue). (C) Cells were double stained for NAV1.8 (SCN10A) (green) and beta-III-tubulin (TUBB3, red). Areas of overlap appear as yellow. All slides were imaged in a Keyence 9000 microscope using a 20× objective. Scale bars = 100 μm.

deficient WA14 cells within the relatively short time span of 12 days (Fig. 5A). Using immunostaining, we confirmed these cells were peripheral-type sensory neurons (Fig. 6) that expressed the pain receptors, NAV1.7, NAV1.8, and TRPV1 (Fig. 7).

It is well known that neuronal cells with fully established neuronal processes are difficult to transfer from the original dish in which they were plated without causing a large amount of irreversible cells damage resulting in variable amounts of cell death. Using a two-step procedure developed by Hoelting et al. [41], we were able to transfer the cells to experimental culture vessels during the differentiation process, before their neuronal phenotype was fully established, resulting in minimal loss of viability (Fig. 5B). In addition, we could viably freeze the partially differentiated cells and continue the differentiation protocol after thawing. This allows the establishment of a cell bank of mutant and wild-type cells at the same stage of differentiation that can be thawed at the same time to be used in comparative studies and drug screening.

In summary, by using CRISPR-Cas9 gene editing techniques we generated two AGA-deficient hESC clones that can be used to create genetically and physiologically relevant cellular models to study the pathogenesis of Fabry disease. To our knowledge, this is the first report demonstrating that AGA-deficient human stem cells can be differentiated to peripheral neurons with nociceptor properties. Since it has been shown that human embryonic stem cells can be differentiated into other cell types such as endothelial cells [55] and monocytes [56], our gene-edited clones can be used to study potential interactions of these other cell types with peripheral neurons in the development of neuropathy in Fabry patients. This human model system offers a new and promising tool for investigating the cellular mechanisms of peripheral neuropathy in Fabry disease and may assist in the development of new therapeutic strategies to help lessen the burden of this disease.

Declaration of Competing Interest

The authors declare that they have no known competing financial interests or personal relationships that could have appeared to influence the work reported in this paper.

Data availability

Data will be made available on request.

Acknowledgements

This research was supported in part by the NIDDK Intramural Research Program and the NINDS Intramural Research Program at the National Institutes of Health, Bethesda, MD, and by Pfizer Inc., New York, NY (grant number #51755565 to UHS). The authors also gratefully acknowledge the help and advice of Prof. Dr. Konrad Sandhoff, The Life & Medical Sciences Institute, University of Bonn, Bonn, Germany. This paper is dedicated to the memory of Dr. Roscoe O. Brady who provided expert advice on the initial stages of the project. He was the authors' colleague and friend for many years, and he is greatly missed.

References

[1] R.O. Brady, A.E. Gal, R.M. Bradley, E. Martensson, A.L. Warshaw, L. Laster, Enzymatic defect in Fabry's disease, N. Engl. J. Med. 276 (1967) 1163–1167, https://doi.org/10.1056/NEJM196705252762101.
[2] R.J. Desnick, Y.A. Ioannou, C.M. Eng, α-Galactosidase A deficiency: Fabry disease, in: A.L. Beaudet, B. Vogelstein, K.W. Kinzler, S.E. Antonarakis, A. Ballabio, K. M. Gibson, G. Mitchell (Eds.), The Online Metabolic and Molecular Bases of Inherited Disease, The McGraw-Hill Companies, Inc., New York, NY, 2014 (accessed September 12, 2017).
[3] T.P. Mechtler, S. Stary, T.F. Metz, V.R. De Jesús, S. Greber-Platzer, A. Pollak, K. R. Herkner, B. Streubel, D.C. Kasper, Neonatal screening for lysosomal storage disorders: feasibility and incidence from a nationwide study in Austria, Lancet 379 (2012) 335–341, https://doi.org/10.1016/S0140-6736(11)61266-X.
[4] Y. Schuller, G.E. Linthorst, C.E.M. Hollak, I.N. Van Schaik, M. Biegstraaten, Pain management strategies for neuropathic pain in Fabry disease - a systematic review, BMC Neurol. 16 (2016) 25, https://doi.org/10.1186/s12883-016-0549-8.
[5] K. MacDermot, A. Holmes, A. Miners, Anderson-Fabry disease: clinical manifestations and impact of disease in a cohort of 98 hemizygous males, J. Med. Genet. 38 (2001) 750–760, https://doi.org/10.1136/jmg.38.11.750.
[6] R. Schiffmann, Neuropathy and Fabry disease: pathogenesis and enzyme replacement therapy, Acta Neurol. Belg. 106 (2006) 61.
[7] O. Morand, J. Johnson, J. Walter, L. Atkinson, G. Kline, A. Frey, J. Politei, R. Schiffmann, Symptoms and quality of life in patients with Fabry disease: results from an international patient survey, Adv. Ther. 36 (2019) 2866–2880, https://doi.org/10.1007/s12325-019-01061-x.
[8] J.N. Rajan, K. Ireland, R. Johnson, K.M. Stepien, Review of mechanisms, pharmacological management, psychosocial implications, and holistic treatment of pain in Fabry disease, J. Clin. Med. 10 (2021) 4168, https://doi.org/10.3390/jcm10184168.
[9] A.J. Burand, C.L. Stucky, Fabry disease pain: patient and preclinical parallels, Pain 162 (2021) 1305–1321, https://doi.org/10.1097/j.pain.0000000000002152.
[10] N. Gadoth, U. Sandbank, Involvement of dorsal root ganglia in Fabry's disease, J. Med. Genet. 20 (1983) 309–312.
[11] S. Jabbarzadeh-Tabrizi, M. Boutin, T.S. Day, M. Taroua, R. Schiffmann, C. Auray-Blais, J.-S. Shen, Assessing the role of glycosphingolipids in the phenotype severity of Fabry disease mouse model, J. Lipid Res. (2020), https://doi.org/10.1194/jlr.RA120000909 jlr.RA120000909.
[12] L. Hofmann, D. Hose, A. Grießhammer, R. Blum, F. Döring, S. Dib-Hajj, S. Waxman, C. Sommer, E. Wischmeyer, N. Üçeyler, Characterization of small fiber pathology

in a mouse model of Fabry disease, ELife 7 (2018), e39300, https://doi.org/10.7554/eLife.39300.
[13] J.J. Miller, K. Aoki, F. Moehring, C.A. Murphy, C.L. O'Hara, M. Tiemeyer, C. L. Stucky, N.M. Dahms, Neuropathic pain in a Fabry disease rat model, JCI Insight 3 (2018), e99171, https://doi.org/10.1172/jci.insight.99171.
[14] R. Sakiri, B. Ramegowda, V.L. Tesh, Shiga toxin type 1 activates tumor necrosis factor-α gene transcription and nuclear translocation of the transcriptional activators nuclear factor-κB and activator Protein-1, Blood 92 (1998) 558–566, https://doi.org/10.1182/blood.V92.2.558.
[15] N. Üçeyler, D. Urlaub, C. Mayer, S. Uehlein, M. Held, C. Sommer, Tumor necrosis factor-α links heat and inflammation with Fabry pain, Mol. Genet. Metab. 127 (2019) 200–206, https://doi.org/10.1016/j.ymgme.2019.05.009.
[16] V. Rickert, D. Kramer, A.-L. Schubert, C. Sommer, E. Wischmeyer, N. Üçeyler, Globotriaosylceramide-induced reduction of KCa1.1 channel activity and activation of the Notch1 signaling pathway in skin fibroblasts of male Fabry patients with pain, Exp. Neurol. 324 (2020), 113134, https://doi.org/10.1016/j.expneurol.2019.113134.
[17] M. Spitzel, E. Wagner, M. Breyer, D. Henniger, M. Bayin, L. Hofmann, D. Mauceri, C. Sommer, N. Üçeyler, Dysregulation of immune response mediators and pain-related ion channels is associated with pain-like behavior in the GLA KO mouse model of fabry disease, Cells. 11 (2022) 1730, https://doi.org/10.3390/cells11111730.
[18] L. Choi, J. Vernon, O. Kopach, M.S. Minett, K. Mills, P.T. Clayton, T. Meert, J. N. Wood, The Fabry disease-associated lipid Lyso-Gb3 enhances voltage-gated calcium currents in sensory neurons and causes pain, Neurosci. Lett. 594 (2015) 163–168, https://doi.org/10.1016/j.neulet.2015.01.084.
[19] A. Tuttolomondo, I. Simonetta, G. Duro, R. Pecoraro, S. Miceli, P. Colomba, C. Zizzo, A. Nucera, M. Daidone, T. Di Chiara, R. Scaglione, V. Della Corte, F. Corpora, D. Vogiatzis, A. Pinto, Inter-familial and intra-familial phenotypic variability in three Sicilian families with Anderson-Fabry disease, Oncotarget 8 (2017) 61415–61424, https://doi.org/10.18632/oncotarget.18250.
[20] A. Tuttolomondo, I. Simonetta, R. Riolo, F. Todaro, T. Di Chiara, S. Miceli, A. Pinto, Pathogenesis and molecular mechanisms of Anderson–Fabry disease and possible new molecular addressed therapeutic strategies, Int. J. Mol. Sci. 22 (2021) 10088, https://doi.org/10.3390/ijms221810088.
[21] B. Namer, K. Ørstavik, R. Schmidt, N. Mair, I.P. Kleggetveit, M. Zeidler, T. Martha, E. Jorum, M. Schmelz, T. Kalpachidou, M. Kress, M. Langeslag, Changes in ionic conductance signature of nociceptive neurons underlying Fabry disease phenotype, Front. Neurol. 8 (2017) 335, https://doi.org/10.3389/fneur.2017.00335.
[22] S.J. Middleton, A.M. Barry, M. Comini, Y. Li, P.R. Ray, S. Shiers, A. C. Themistocleous, M.L. Uhelski, X. Yang, P.M. Dougherty, T.J. Price, D.L. Bennett, Studying human nociceptors: from fundamentals to clinic, Brain. 144 (2021) 1312–1335, https://doi.org/10.1093/brain/awab048.
[23] J.-M. Itier, G. Ret, S. Viale, L. Sweet, D. Bangari, A. Caron, F. Le-Gall, B. Bénichou, J. Leonard, J.-F. Deleuze, C. Orsini, Effective clearance of GL-3 in a human iPSC-derived cardiomyocyte model of Fabry disease, J. Inherit. Metab. Dis. 37 (2014) 1013–1022, https://doi.org/10.1007/s10545-014-9724-5.
[24] S. Kawagoe, T. Higuchi, M. Otaka, Y. Shimada, H. Kobayashi, H. Ida, T. Ohashi, H. J. Okano, M. Nakanishi, Y. Eto, Morphological features of iPS cells generated from Fabry disease skin fibroblasts using Sendai virus vector (SeVdp), Mol. Genet. Metab. 109 (2013) 386–389, https://doi.org/10.1016/j.ymgme.2013.06.003.
[25] A.J. Duarte, D. Ribeiro, R. Santos, L. Moreira, J. Bragança, O. Amaral, Induced pluripotent stem cell line (INSAi002-A) from a Fabry disease patient hemizygote for the rare p.W287X mutation, Stem Cell Res. 45 (2020), 101794, https://doi.org/10.1016/j.scr.2020.101794.
[26] T. Klein, K. Günther, C.K. Kwok, F. Edenhofer, N. Üçeyler, Generation of the human induced pluripotent stem cell line (UKWNLi001-A) from skin fibroblasts of a woman with Fabry disease carrying the X-chromosomal heterozygous c.708 G > C (W236C) missense mutation in exon 5 of the alpha-galactosidase–A gene, Stem Cell Res. 31 (2018) 222–226, https://doi.org/10.1016/j.scr.2018.08.009.
[27] S. Cui, Y.J. Shin, E.J. Ko, S.W. Lim, J.H. Ju, K.I. Lee, J.Y. Lee, C.W. Yang, B. H. Chung, Human-induced pluripotent stem cell lines (CMCi006-A and CMCi007-A) from a female and male patient with Fabry disease carrying the same frameshift deletion mutation, Stem Cell Res. 51 (2021), 102214, https://doi.org/10.1016/j.scr.2021.102214.
[28] Y. Chien, S.-J. Chou, Y.-L. Chang, H.-B. Leu, Y.-P. Yang, P.-H. Tsai, Y.-H. Lai, K.-H. Chen, W.-C. Chang, S.-H. Sung, W.-C. Yu, Inhibition of Arachidonate 12/15-lipoxygenase improves α-galactosidase efficacy in iPSC-derived cardiomyocytes from Fabry patients, IJMS. 19 (2018) 1480, https://doi.org/10.3390/ijms19051480.
[29] Y. Zhu, L. Zhang, G. Wang, J. Zhao, X. Hou, H. Wu, Y. Xu, J. Mao, Z. Liu, J. Zhang, Generation of an induced pluripotent stem cell line (ZJUi007-A) from a 11-year-old patient of Fabry disease, Stem Cell Res. 55 (2021), 102475, https://doi.org/10.1016/j.scr.2021.102475.
[30] S.-J. Chou, W.-C. Yu, Y.-L. Chang, W.-Y. Chen, W.-C. Chang, Y. Chien, J.-C. Yen, Y.-Y. Liu, S.-J. Chen, C.-Y. Wang, Y.-H. Chen, D.-M. Niu, S.-J. Lin, J.-W. Chen, S.-H. Chiou, H.-B. Leu, Energy utilization of induced pluripotent stem cell-derived cardiomyocyte in Fabry disease, Int. J. Cardiol. 232 (2017) 255–263, https://doi.org/10.1016/j.ijcard.2017.01.009.
[31] H. Kilpinen, A. Goncalves, A. Leha, V. Afzal, K. Alasoo, S. Ashford, S. Bala, D. Bensaddek, F.P. Casale, O.J. Culley, P. Danecek, A. Faulconbridge, P. W. Harrison, A. Kathuria, D. McCarthy, S.A. McCarthy, R. Meleckyte, Y. Memari, N. Moens, F. Soares, A. Mann, I. Streeter, C.A. Agu, A. Alderton, R. Nelson, S. Harper, M. Patel, A. White, S.R. Patel, L. Clarke, R. Halai, C.M. Kirton, A. Kolb-Kokocinski, P. Beales, E. Birney, D. Danovi, A.I. Lamond, W.H. Ouwehand, L. Vallier, F.M. Watt, R. Durbin, O. Stegle, D.J. Gaffney, Common genetic variation drives molecular heterogeneity in human iPSCs, Nature. 546 (2017) 370–375, https://doi.org/10.1038/nature22403.
[32] F. Rouhani, N. Kumasaka, M.C. de Brito, A. Bradley, L. Vallier, D. Gaffney, Genetic background drives transcriptional variation in human induced pluripotent stem cells, PLoS Genet. 10 (2014), e1004432, https://doi.org/10.1371/journal.pgen.1004432.
[33] V. Volpato, C. Webber, Addressing variability in iPSC-derived models of human disease: guidelines to promote reproducibility, Dis. Model. Mech. 13 (2020) dmm042317, https://doi.org/10.1242/dmm.042317.
[34] S.M. Chambers, Y. Qi, Y. Mica, G. Lee, X.-J. Zhang, L. Niu, J. Bilsland, L. Cao, E. Stevens, P. Whiting, S.-H. Shi, L. Studer, Combined small-molecule inhibition accelerates developmental timing and converts human pluripotent stem cells into nociceptors, Nat. Biotechnol. 30 (2012) 715–720, https://doi.org/10.1038/nbt.2249.
[35] S.M. Chambers, Y. Mica, G. Lee, L. Studer, M.J. Tomishima, Dual-SMAD inhibition/WNT activation-based methods to induce neural crest and derivatives from human pluripotent stem cells, in: K. Turksen (Ed.), Human Embryonic Stem Cell Protocols, Springer, New York, New York, NY, 2013, pp. 329–343, https://doi.org/10.1007/7651_2013_59.
[36] G.T. Young, A. Gutteridge, H.D. Fox, A.L. Wilbrey, L. Cao, L.T. Cho, A.R. Brown, C. L. Benn, L.R. Kammonen, J.H. Friedman, M. Bictash, P. Whiting, J.G. Bilsland, E. B. Stevens, Characterizing human stem cell–derived sensory neurons at the single-cell level reveals their ion channel expression and utility in pain research, Mol. Ther. 22 (2014) 1530–1543, https://doi.org/10.1038/mt.2014.86.
[37] S. Viventi, M. Dottori, Modelling the dorsal root ganglia using human pluripotent stem cells: a platform to study peripheral neuropathies, Int. J. Biochem. Cell Biol. 100 (2018) 61–68, https://doi.org/10.1016/j.biocel.2018.05.005.
[38] J. Beers, D.R. Gulbranson, N. George, L.I. Siniscalchi, J. Jones, J.A. Thomson, G. Chen, Passaging and colony expansion of human pluripotent stem cells by enzyme-free dissociation in chemically defined culture conditions, Nat. Protoc. 7 (2012) 2029–2040, https://doi.org/10.1038/nprot.2012.130.
[39] C.R. Kaneski, R. Schiffmann, R.O. Brady, G.J. Murray, Use of lissamine rhodamine ceramide trihexoside as a functional assay for alpha-galactosidase A in intact cells, J. Lipid Res. 51 (2010) 2808–2817, https://doi.org/10.1194/jlr.D007294.
[40] J.S. Mayes, Julia B. Scheerer, Richard N. Sifers, Mark L. Donaldson, Differential assay for lysosomal alpha-galactosidases in human tissues and its application to Fabry's disease, Clinical Chemica Acta. 112 (1981) 247–251.
[41] L. Hoelting, S. Klima, C. Karreman, M. Grinberg, J. Meisig, M. Henry, T. Rotshteyn, J. Rahnenführer, N. Blüthgen, A. Sachinidis, T. Waldmann, M. Leist, Stem cell-derived immature human dorsal root ganglia neurons to identify peripheral neurotoxicants: peripheral neurons for drug safety testing, Stem Cells Transl. Med. 5 (2016) 476–487, https://doi.org/10.5966/sctm.2015-0108.
[42] H. Liu, C. Ren, B. Zhu, L. Wang, W. Liu, J. Shi, J. Lin, X. Xia, F. Zeng, J. Chen, X. Jiang, High-efficient transfection of human embryonic stem cells by single-cell plating and starvation, Stem Cells Dev. 25 (2016) 477–491, https://doi.org/10.1089/scd.2015.0301.
[43] B. Steyer, Q. Bu, E. Cory, K. Jiang, S. Duong, D. Sinha, S. Steltzer, D. Gamm, Q. Chang, K. Saha, Scarless genome editing of human pluripotent stem cells via transient puromycin selection, Stem Cell Reports. 10 (2018) 642–654, https://doi.org/10.1016/j.stemcr.2017.12.004.
[44] M.R. Gerrero, R.J. McEvilly, E. Turner, C.R. Lin, S. O'Connell, K.J. Jenne, M. V. Hobbs, M.G. Rosenfeld, Brn-3.0: a POU-domain protein expressed in the sensory, immune, and endocrine systems that functions on elements distinct from known octamer motifs, Proc. Natl. Acad. Sci. U. S. A. 90 (1993) 10841–10845.
[45] Y. Sun, I.M. Dykes, X. Liang, S.R. Eng, S.M. Evans, E.E. Turner, A central role for Islet1 in sensory neuron development linking sensory and spinal gene regulatory programs, Nat. Neurosci. 11 (2008) 1283–1293, https://doi.org/10.1038/nn.2209.
[46] C.R. Kaneski, R.O. Brady, J.A. Hanover, U.H. Schueler, Development of a model system for neuronal dysfunction in Fabry disease, Mol. Genet. Metab. 119 (2016) 144–150, https://doi.org/10.1016/j.ymgme.2016.07.010.
[47] Song, Chien, Yarmishyn, Chou, Yang, Wang, Wang, Leu, Yu, Chang, Chiou, Generation of GLA-knockout human embryonic stem cell lines to model autophagic dysfunction and exosome secretion in fabry disease-associated hypertrophic cardiomyopathy, Cells 8 (2019) 327, https://doi.org/10.3390/cells8040327.
[48] Y.-K. Kim, J.H. Yu, S.-H. Min, S.-W. Park, Generation of a GLA knock-out human-induced pluripotent stem cell line, KSBCi002-A-1, using CRISPR/Cas9, Stem Cell Res. 42 (2020), 101676, https://doi.org/10.1016/j.scr.2019.101676.
[49] J.W. Kim, H.W. Kim, S.A. Nam, J.Y. Lee, H.J. Cho, T.-M. Kim, Y.K. Kim, Human kidney organoids reveal the role of glutathione in Fabry disease, Exp. Mol. Med. 53 (2021) 1580–1591, https://doi.org/10.1038/s12276-021-00683-y.
[50] M.J. Birket, S. Raibaud, M. Lettieri, A.D. Adamson, V. Letang, P. Cervello, N. Redon, G. Ret, S. Viale, B. Wang, B. Biton, J.-C. Guillemot, V. Mikol, J. P. Leonard, N.A. Hanley, C. Orsini, J.-M. Itier, A human stem cell model of Fabry disease implicates LIMP-2 accumulation in cardiomyocyte pathology, Stem Cell Reports. 13 (2019) 380–393, https://doi.org/10.1016/j.stemcr.2019.07.004.
[51] H.-S. Do, S.-W. Park, I. Im, D. Seo, H.-W. Yoo, H. Go, Y.H. Kim, G.Y. Koh, B.-H. Lee, Y.-M. Han, Enhanced thrombospondin-1 causes dysfunction of vascular endothelial cells derived from Fabry disease-induced pluripotent stem cells, EBioMedicine. 52 (2020), 102633, https://doi.org/10.1016/j.ebiom.2020.102633.
[52] Y. Kuramoto, A.T. Naito, H. Tojo, T. Sakai, M. Ito, M. Shibamoto, A. Nakagawa, T. Higo, K. Okada, T. Yamaguchi, J.-K. Lee, S. Miyagawa, Y. Sawa, Y. Sakata, I. Komuro, Generation of Fabry cardiomyopathy model for drug screening using induced pluripotent stem cell-derived cardiomyocytes from a female Fabry patient, J. Mol. Cell. Cardiol. 121 (2018) 256–265, https://doi.org/10.1016/j.yjmcc.2018.07.246.

[53] S. Kim, D. Kim, S.W. Cho, J. Kim, J.-S. Kim, Highly efficient RNA-guided genome editing in human cells via delivery of purified Cas9 ribonucleoproteins, Genome Res. 24 (2014) 1012–1019, https://doi.org/10.1101/gr.171322.113.
[54] L.A. McDermott, G.A. Weir, A.C. Themistocleous, A.R. Segerdahl, I. Blesneac, G. Baskozos, A.J. Clark, V. Millar, L.J. Peck, D. Ebner, I. Tracey, J. Serra, D. L. Bennett, Defining the functional role of NaV1.7 in human nociception, Neuron. 101 (2019) 905–919.e8, https://doi.org/10.1016/j.neuron.2019.01.047.
[55] G. Balconi, R. Spagnuolo, E. Dejana, Development of endothelial cell lines from embryonic stem cells: a tool for studying genetically manipulated endothelial cells in vitro, ATVB. 20 (2000) 1443–1451, https://doi.org/10.1161/01.ATV.20.6.1443.
[56] K.R. Karlsson, S. Cowley, F.O. Martinez, M. Shaw, S.L. Minger, W. James, Homogeneous monocytes and macrophages from human embryonic stem cells following coculture-free differentiation in M-CSF and IL-3, Exp. Hematol. 36 (2008) 1167–1175, https://doi.org/10.1016/j.exphem.2008.04.009.